Biochimica et Biophysica Acta 1837 (2014) 1012–1018

Contents lists available at ScienceDirect

Biochimica et Biophysica Acta

journal homepage: www.elsevier.com/locate/bbabio

# Reaction of wild-type and Glu243Asp variant yeast cytochrome *c* oxidase with $O_2$ ☆,☆☆

Linda Näsvik Öjemyr [a], Amandine Maréchal [b], Henrik Vestin [a], Brigitte Meunier [c], Peter R. Rich [b], Peter Brzezinski [a,*]

[a] Department of Biochemistry and Biophysics, The Arrhenius Laboratories for Natural Sciences, Stockholm University, SE-106 91 Stockholm, Sweden
[b] Glynn Laboratory of Bioenergetics, Institute of Structural and Molecular Biology, University College London, Gower Street, London WC1E 6BT, UK
[c] Centre de Génétique Moléculaire du CNRS, UPR 3404, avenue de la Terrasse, 91198 Gif-sur-Yvette Cedex, France

ARTICLE INFO

*Article history:*
Received 5 December 2013
Received in revised form 7 March 2014
Accepted 21 March 2014
Available online 28 March 2014

*Keywords:*
Electron transfer
Membrane protein
Respiration
Redox reaction
Metalloprotein
Cytochrome $aa_3$

ABSTRACT

We have studied internal electron transfer during the reaction of *Saccharomyces cerevisiae* mitochondrial cytochrome *c* oxidase with dioxygen. Similar absorbance changes were observed with this yeast oxidase as with the previously studied *Rhodobacter sphaeroides* and bovine mitochondrial oxidases, which suggests that the reaction proceeds along the same trajectory. However, notable differences were observed in rates and electron-transfer equilibrium constants of specific reaction steps, for example the ferryl (**F**) to oxidized (**O**) reaction was faster with the yeast (0.4 ms) than with the bovine oxidase (~1 ms) and a larger fraction $Cu_A$ was oxidized with the yeast than with the bovine oxidase in the peroxy ($\mathbf{P_R}$) to **F** reaction. Furthermore, upon replacement of Glu243, located at the end of the so-called D proton pathway, by Asp the $\mathbf{P_R} \rightarrow \mathbf{F}$ and $\mathbf{F} \rightarrow \mathbf{O}$ reactions were slowed by factors of ~3 and ~10, respectively, and electron transfer from $Cu_A$ to heme *a* during the $\mathbf{P_R} \rightarrow \mathbf{F}$ reaction was not observed. These data indicate that during reduction of dioxygen protons are transferred through the D pathway, via Glu243, to the catalytic site in the yeast mitochondrial oxidase. This article is part of a Special Issue entitled: 18th European Bioenergetic Conference.



## 1. Introduction

In aerobic organisms electrons that are extracted from nutrients are transferred via a series of membrane bound respiratory chain proteins to dioxygen. The free energy is conserved by translocation or pumping of protons (or in some cases sodium ions) across the membrane and stored in the electrochemical proton gradient. This is used, for example, for transmembrane transport or synthesis of ATP. In mammalian and *Saccharomyces* (*S.*) *cerevisiae* yeast mitochondria, $O_2$ reduction is catalyzed by cytochrome *c* oxidases (CytcOs) with electrons delivered by cytochrome *c*. The first electron acceptor from cytochrome *c* is $Cu_A$, found in SU II, and electrons are then transferred within SU I via heme *a* to the bimetallic catalytic oxygen-binding site, consisting of heme $a_3$ and $Cu_B$. These heme-copper oxidases are members of a diverse range of homologous oxidoreductases [1,2]. The mammalian and *S. cerevisiae* CytcOs belong to the large A-class of oxidases, which also includes $aa_3$-type CytcOs from many bacteria such as *Rhodobacter sphaeroides* and *Paracoccus denitrificans* [1,2]. Their $O_2$ reduction reaction is energetically linked to proton pumping across the membrane, from the negative (*n*) side to the positive (*p*) side, with a typical stoichiometry of one pumped proton per electron transferred to $O_2$.

In the bacterial A-class oxidases, two proton pathways, denoted by letters D (after a conserved Asp residue at the orifice) and K (after a conserved Lys residue within the pathway), have been identified based on functional and structural studies. The K pathway transfers 1–2 protons upon reduction of the catalytic site, while the D pathway transfers the remaining substrate protons to the catalytic site as well as all pumped protons. The structure and function of CytcO have been reviewed, for example, in [3–12].

To date most investigations of the mitochondrial CytcOs have been performed with bovine heart CytcO (*Bos taurus*, *Bt*CytcO). However, in recent years *S. cerevisiae* yeast CytcO (*Sc*CytcO) has emerged as a model mitochondrial CytcO in which effects of mutations on function can be studied [13,14] (Fig. 1A). Both D and K pathways are conserved between these two CytcOs, apart from minor differences that are unlikely to be functionally relevant [13]. In *Sc*CytcO the D pathway starts near Asp92 (corresponding to Asp132 in the *R. sphaeroides* CytcO (*Rs*CytcO)

*Abbreviations:* CytcO, cytochrome *c* oxidase; *n* side, negative side of the membrane; *p* side, positive side of the membrane; **R**, the four-electron reduced CytcO; **A**, reduced CytcO with $O_2$ bound to heme $a_3$; $\mathbf{P_R}$, the "peroxy" state formed after transfer of a third electron to the catalytic site; **F**, the ferryl state formed at the catalytic site after protonation of $\mathbf{P_R}$; **O**, the oxidized CytcO; SU, subunit; WT, wild-type

☆ This article is part of a Special Issue entitled: 18th European Bioenergetic Conference.
☆☆ Funding: These studies were supported by grants from the Swedish Research Council (grant number 2010-4987), the Knut and Alice Wallenberg Foundation, the Biotechnology and Biological Sciences Research Council (grant number BB/K001094/1) and EU COST Action 0902.

* Corresponding author. Tel.: +46 70 609 2642; fax: +46 8 153679.
*E-mail address:* peterb@dbb.su.se (P. Brzezinski).

http://dx.doi.org/10.1016/j.bbabio.2014.03.012
0005-2728/

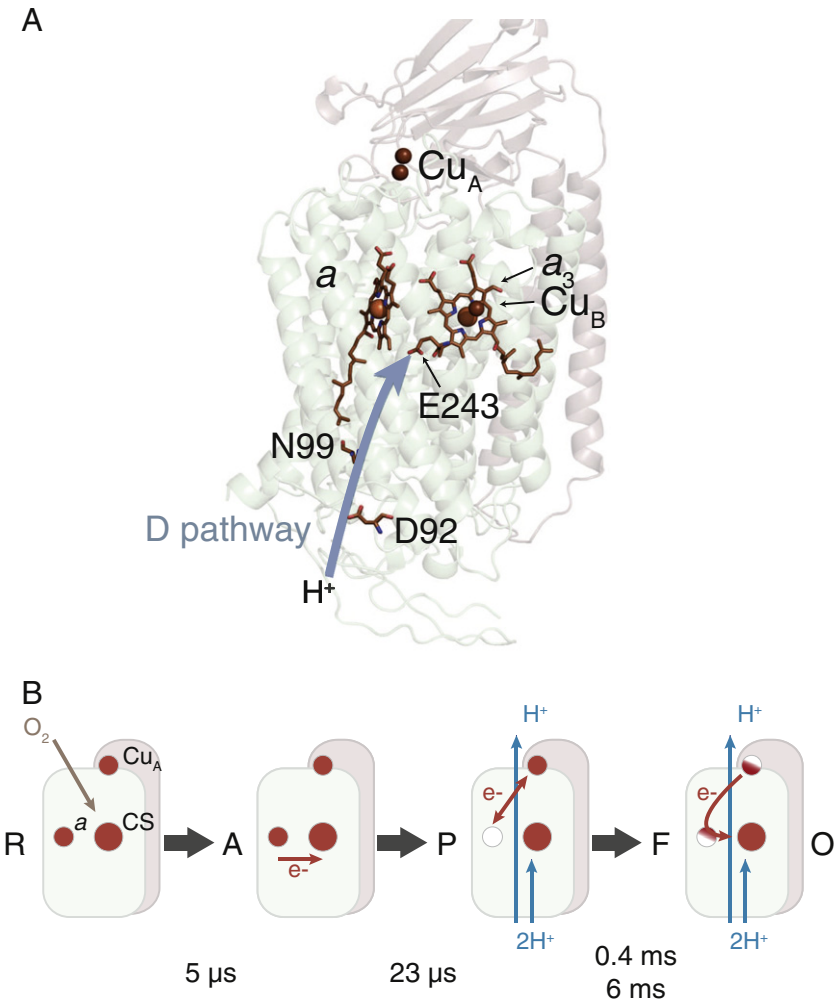


**Fig. 1.** (A) A structural model of subunits I and II of the *Sc*CytcO, based on the X-ray crystal structure of the equivalent subunits of the bovine mitochondrial enzyme. Shown is the D pathway used for proton uptake during $O_2$ reduction. (B) A schematic illustration of the reaction of the reduced oxidase with $O_2$, based on earlier results with e.g. the *Rs*CytcO and *Bt*CytcO. The filled and empty circles represent the reduced and oxidized redox centers, respectively. Flash photolysis of CO from the four-electron reduced CytcO yields the reduced enzyme, **R** (CS is the catalytic site, i.e. heme $a_3$ and $Cu_B$). Binding of $O_2$ to heme $a_3$ results in formation of **A**. Next, an electron is transferred from heme *a* to the catalytic site forming state $\mathbf{P_R}$. During the $\mathbf{P_R} \rightarrow \mathbf{F}$ reaction at the catalytic site there is a fractional electron transfer from $Cu_A$ to heme *a*, proton uptake to the catalytic site and proton pumping across the membrane. Finally, in the last step of the reaction the electron from the $Cu_A$–heme *a* equilibrium is transferred to the catalytic site, linked to proton uptake and proton pumping across the membrane. The time constants are from the present study.

and Asp91 in *Bt*CytcO) at the *n* side of the membrane and spans a distance of ~25 Å towards the *p* side to Glu243 (Glu286 and Glu242 in the *R. sphaeroides* and bovine CytcOs, respectively). In *Bt*CytcO a third, H (His) pathway was suggested to be used for the transfer of the pumped protons [15–17]. Although there are structural differences between the *Sc*CytcO and *Bt*CytcO at the entry and exit regions of the H pathway, the membrane-spanning part appears to be similar [13,14]. This pathway is less obvious in the bacterial CytcOs and substitution of amino acids at positions equivalent to those of the H pathway in the *Bt*CytcO indicated that these residues are not involved in proton transfer [18,19].

The kinetics of electron transfer and associated proton uptake through the D pathway have been investigated, for example, using a "flow-flash" approach that involves pre-reduction of all metal sites in the presence of carbon monoxide (CO), which binds to heme $a_3$, followed by flash photolysis of the CO ligand after addition of $O_2$ (for review, see [7,8,10,20–22]) (Fig. 1B). $O_2$ binds with a time constant of ~10 µs at 1 mM $O_2$ to form ferrous-oxo compound **A**, followed in time by electron transfer from heme *a* to the catalytic site with a time constant of 30–70 µs (depending on the CytcO source). This results in O – O bond cleavage and formation of a ferryl intermediate that displays an absorption maximum at 607 nm, termed $\mathbf{P_R}$. In the next step, two protons are taken up from the *n*-side solution; one is transferred to the catalytic site to form the ferryl state (termed **F**) with an absorption maximum at 580 nm while the other is transferred through a "pump site" (presumably located "above" the hemes) and into to the *p*-side aqueous phase. In the bacterial A-type oxidases, both of these protons are thought to be transferred through the D pathway to Glu286 (*Rs*CytcO numbering, Glu243 in *Sc*CytcO), which is the branching point for connection to both the catalytic site and the proton exit pathways. Both proton uptake reactions and proton release to the *p*-side display the same time constant of ~100 µs at pH 7 [23,24]. Over the same timescale there is a fractional electron transfer from $Cu_A$ to heme *a*. Finally, the remaining electron in the equilibrated $Cu_A$–heme *a* is transferred with a time constant of ~1 ms into the catalytic site, converting the **F** state into the oxidized (**O**) form. As for the $\mathbf{P_R} \rightarrow \mathbf{F}$ reaction, this $\mathbf{F} \rightarrow \mathbf{O}$ step is also linked in time to the uptake of two protons from the *n* side and release of one pumped proton to the *p* side.

With the bacterial A-type oxidases replacement of either Asp132 or Glu286 (*Rs*CytcO numbering; Asp92 or Glu243, in *Sc*CytcO) by non-protonatable analogs Asn or Gln, respectively, results in almost a complete loss of enzymatic activity and impaired proton uptake from

solution. In the Glu286Gln variant *Rs*CytcO [25] and *P. denitrificans* CytcO [26] the reaction stops at the $\mathbf{P_R}$ state because the internal proton donor (i.e. Glu286) to the catalytic site is absent. In contrast, in the Asp132Asn structural variant (in which the entrance to the D pathway is blocked) the $\mathbf{P_R} \rightarrow \mathbf{F}$ reaction still occurs because Glu286 can still donate a proton to the catalytic site; the reaction stops at **F** because re-protonation of Glu286 from the *n*-side solution is blocked [27].

Substitution of residues Glu243 and Asp92 (Fig. 1A) in the D pathway of the *Sc*CytcO resulted in lowered respiratory growth [14], which indicates that the D pathway is also involved in proton transfer in this mitochondrial CytcO. Furthermore, the Glu243Asp CytcO displayed a catalytic activity of 50% of that of the wild-type CytcO [14], which is similar to the decreases found with *R. sphaeroides* CytcO (~50%) [28], *P. denitrificans* CytcO (~60%) [29] and the *Escherichia coli* quinol oxidase (80%) [30]. The two latter Asp variant bacterial oxidases pump protons with a stoichiometry similar to that of the wild-type CytcO [29,30].

This study addresses two issues, motivated by suggested differences in the roles of the D pathway for the mitochondrial and bacterial A-type CytcOs: (*i*) a comparison of the reaction rates of the *Sc*CytcO and other A-class oxidases studied earlier; and (*ii*) an analysis of the origin of the lower Glu243Asp variant activity and the role of the D pathway in the mitochondrial *Sc*CytcO.

## 2. Materials and methods

### 2.1. Growth and purification

*S. cerevisiae* strains 6H-WT and 6H-E243D$_I$, constructed as described in [14] were grown in YPGal media and His-tagged CytcO wild-type and Glu243Asp variant were purified as described in [14].

### 2.2. Preparation of fully reduced CO bound ScCytcO

The enzyme buffer was exchanged for 5 mM Tris pH 8.5, 0.05% DDM, 100 μM EDTA by concentration and dilution cycles (Amicon Ultra, 15 ml, 100 kDa). The samples were transferred to Thunberg cuvettes and, after exchange of the atmosphere in the cuvette to nitrogen, the *Sc*CytcO was reduced by 2 mM ascorbate and 1 μM PMS. The extent of reduction of the hemes was monitored spectrophotometrically (Cary 400, Varian), and when the *Sc*CytcO was fully reduced the atmosphere was exchanged with CO.

### 2.3. Flow-flash measurement

Fully reduced CO-bound *Sc*CytcO was rapidly mixed in a stopped-flow apparatus with an oxygen-saturated buffer, 100 mM HEPES pH 7.5, 0.05% DDM and 100 μM EDTA, at a ratio of 1:5 or 1:2.5 for the wild-type and Glu243Asp *Sc*CytcO, respectively. The CO ligand was dissociated by a ~10-ns laser flash (532 nm, Quantel Brilliant Nd-YAG) 200–300 ms after mixing. This ligand dissociation allowed oxygen to bind to heme $a_3$. The subsequent oxidation of *Sc*CytcO was monitored by measuring absorbance changes as a function of time at several wavelengths (see figure legends).

To investigate the H/D kinetic isotope effect (KIE), experiments were performed with buffer and reactant solutions prepared with $D_2O$. The enzyme buffer solution was exchanged for 1 mM Tris, 100 μM EDTA and 0.05% DDM at a pH reading of 8.5 (see explanation why the pH-meter reading and not pD is relevant here [31,32]) by concentration dilution cycles (Amicon Ultra 15 ml). The enzyme was reduced under an atmosphere of $N_2$ with 2 mM ascorbate and 1 μM hexaaminoruthenium(III) chloride, both added from stocks in $D_2O$. The fully reduced CO-bound enzyme was mixed 1:1 with 100 mM HEPES at a pH-meter reading of 7.5, 100 μM EDTA and 0.05% DDM. The pH-meter reading after mixing was 7.5.

## 3. Results

### 3.1. Handling of the ScCytcO

Some of the *Sc*CytcO preparations precipitated slowly when left at pH 7.5 at room temperature for extended periods, possibly due to delipidation of the protein during purification or to the presence of the 6-His tag. However, all preparations were stable at pH 8.5, even at a relatively low buffer concentration. Consequently, the *Sc*CytcO–CO complex was generated in an anaerobic solution at pH 8.5 with a low buffer concentration and mixed with an $O_2$-containing solution at a high buffer concentration at pH 7.5 (with v:v ratios between 1:1 and 1:5, see the "Materials and methods"). The data obtained using this method were the same as those obtained with a stable *Sc*CytcO preparation at pH 7.5 mixed with an $O_2$-containing solution at the same pH.

### 3.2. Reaction of the fully reduced wild type ScCytcO with oxygen

The black traces in Fig. 2 show the absorbance changes at different wavelengths upon photolysis 200–300 ms after mixing the fully reduced CO-bound wild-type enzyme with an oxygen-saturated buffer at pH 7.5. These follow the same general pattern as with the well-characterized *Bt*CytcO and the bacterial A-type CytcOs (see the Introduction) and so can be interpreted in terms of specific electron and proton transfer reactions with the assumption that qualitatively the same reactions occur. Dissociation of CO from the reduced heme $a_3$ at the time of the flash ($t = 0$) resulted in an initial rapid absorbance increase at 445 nm (Fig. 2A). This was followed by a rapid decrease in absorbance at 445 nm associated with oxygen binding to the reduced heme $a_3$ ($\mathbf{R} \rightarrow \mathbf{A}$) with a time constant of ~5 μs at ~1 mM $O_2$. After binding of $O_2$, a further decrease in absorbance at 445 nm occurred with a time constant of ~23 μs (Fig. 2A). This reaction was also associated with a small decrease in absorbance at 580 nm (Fig. 2B) and can be presumed to be associated with the $\mathbf{A} \rightarrow \mathbf{P_R}$ reaction involving electron transfer from heme *a* to the catalytic site to form state $\mathbf{P_R}$. The $\mathbf{A} \rightarrow \mathbf{P_R}$ step is also seen at 595 nm (not shown). At 445 nm the $\mathbf{A} \rightarrow \mathbf{P_R}$ step is followed by a small lag phase associated with electron transfer to heme *a* during the $\mathbf{P_R} \rightarrow \mathbf{F}$ reaction (see below), which masks part of the 23-μs $\mathbf{A} \rightarrow \mathbf{P_R}$ absorbance decrease. The time constant for $\mathbf{P_R}$ formation was about the same as that in *Bt*CytcO (~25 μs) and a factor of two faster than that in *Rs*CytcO (~55 μs) [33].

Assuming that the reaction sequence is the same as that determined for the bacterial A-type oxidases, in the next ($\mathbf{P_R} \rightarrow \mathbf{F}$) phase a proton is transferred to the catalytic site to form the ferryl (**F**) state and a further proton is ejected into the *p* phase. Both protons should be transferred through Glu243, with Glu243 being reprotonated each time by proton uptake through the D pathway from the *n*-side solution [34]. At the same time the last (fourth) electron at $Cu_A$ equilibrates with heme *a*. Reduction of heme *a* and formation of **F** both contribute small absorbance increases, seen only as lag phases, at 445 nm and 580 nm respectively (Fig. 2A, B) in the 100–200 μs time range. This $\mathbf{P_R} \rightarrow \mathbf{F}$ step is most clearly seen at 830 nm (Fig. 2C) where oxidation of $Cu_A$ results in an increase in absorbance with a time constant of ~90 μs (~70% of the total amplitude).

In the final step of the reaction, the fourth electron is transferred from the equilibrated $Cu_A$–heme *a* into the catalytic site to form the oxidized (**O**) state. As in the $\mathbf{P_R} \rightarrow \mathbf{F}$ step, this electron transfer is also linked in time to proton transfer from Glu243 to the catalytic site as well as to a proton translocation across the structure and with rapid reprotonation of the Glu243 from the *n* phase. This $\mathbf{F} \rightarrow \mathbf{O}$ reaction was associated with a biphasic decrease in absorbance at 445 nm due to heme *a* oxidation (Fig. 2A) with a main component (84%; $\tau \cong 0.4$ ms) and a minor component (16%; $\tau \cong 6$ ms) (a one-component fit gave an overall time constant of ~0.6 ms). The $\mathbf{F} \rightarrow \mathbf{O}$ reaction is also linked to a decrease in

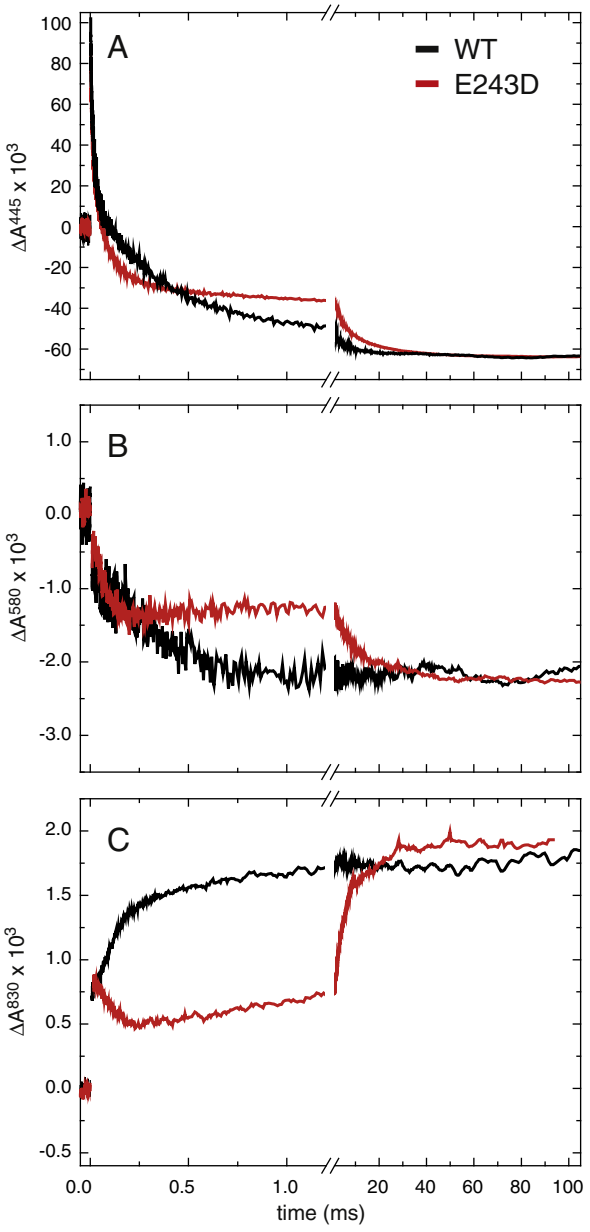


**Fig. 2.** Absorbance changes associated with reaction of the reduced wild-type (WT, black) and Glu243Asp (E243D, red) mutant *Sc*CytcO, and $O_2$. (A) At 445 nm the absorbance increase at time = 0 is associated with dissociation of CO from the reduced heme $a_3$. It is followed in time by a decrease in absorbance associated with binding of $O_2$ (decrease to about $\Delta A = 0$) and electron transfer from heme *a* to the catalytic site forming $\mathbf{P_R}$, although this absorbance change is masked by absorbance changes associated with the next step of the reaction. The $\mathbf{P_R} \rightarrow \mathbf{F}$ reaction is seen as a small lag phase in the time range ~100 μs–300 μs (this lag phase is distinguishable here upon comparison of the wild-type and Glu243Asp, mainly because it is not seen with the structural variant CytcO). The slowest decrease in absorbance is associated with final oxidation of the CytcO ($\mathbf{F} \rightarrow \mathbf{O}$); (B) At 580 nm the initial decrease in absorbance is associated with oxidation of heme *a* forming $\mathbf{P_R}$. The lag phase in the time range ~100 μs–200 μs is associated with the $\mathbf{P_R} \rightarrow \mathbf{F}$ reaction. This component is more clearly seen with the structural variant of the CytcO as an increase in absorbance over a time scale 200 μs–1 ms. The final decrease in absorbance is associated with the $\mathbf{F} \rightarrow \mathbf{O}$ reaction. (C) At 830 nm the absorbance change at $t = 0$ is associated with CO dissociation. The increase in absorbance at $t > 0$ is associated with oxidation of $Cu_A$. Experimental conditions after mixing: 80 mM HEPES at pH 7.5, 100 μM EDTA, 0.05% DDM, and 1 mM and 0.9 mM $O_2$ for the wild type and Glu243Asp samples, respectively. Traces have been scaled to 1 μM of reacting enzyme and the wild type traces at 445 have been multiplied by 1.35 to get the same final oxidation level.

absorbance at 580 nm ($\tau \cong 0.5$ ms, Fig. 2C) due to ferryl heme reduction, and an increase at 830 nm due to oxidation of the remaining ~30% $Cu_A$ with a time constant of ~0.6 ms.

### 3.3. Reaction of the fully reduced ScCytcO Glu243Asp variant with oxygen

In the Glu243Asp mutant *Sc*CytcO electron transfer from heme *a* to the catalytic site during the $\mathbf{A} \rightarrow \mathbf{P_R}$ reaction was slowed by a factor of ~3 ($\tau \cong 80$ μs). This component is seen as a decrease in absorbance at 445 nm (Fig. 2A, red traces at $t = 0$–0.25 ms and $\Delta A = -30$–0). As indicated above, for the wild-type CytcO the $\mathbf{A} \rightarrow \mathbf{P_R}$ decrease in absorbance is masked by an increase associated with re-reduction of heme *a* and it is therefore difficult to directly compare the wild-type and Glu243Asp traces. The subsequent increase in absorbance at 580 nm (Fig. 2B) is associated with the $\mathbf{P_R} \rightarrow \mathbf{F}$ reaction and displayed a time constant of ~300 μs, which is significantly slower than that for the wild-type CytcO ($\tau \cong 90$ μs). As outlined above, the $\mathbf{P_R} \rightarrow \mathbf{F}$ reaction in the wild-type *Sc*CytcO is associated with electron transfer from $Cu_A$ to heme *a*. With the Glu243Asp variant this electron transfer was not observed, i.e. $Cu_A$ remained reduced during the $\mathbf{P_R} \rightarrow \mathbf{F}$ reaction (Fig. 2C, red trace).

The final $\mathbf{F} \rightarrow \mathbf{O}$ reaction resulted in absorbance decay at 445 nm, and again displayed two components with time constants of ~2 ms and ~15 ms, respectively, with approximately equal extents (Fig. 2A). Thus, the contribution from the slow component was significantly larger than that for the wild-type *Sc*CytcO. Two kinetic components were also observed at 830 nm (Fig. 2C) with approximately the same time constants as those at 445 nm, with amplitude contributions of ~65% and ~35%, respectively.

### 3.4. Deuterium isotope effects on the A to P and F to O transitions

The experiments at 445 nm described above were repeated in $D_2O$ at a pH meter reading of 7.5 (Fig. 3, blue and green traces for the wild-type and Glu243Asp variant, respectively). Previous studies with e.g. the *Bt*CytcO showed that the $\mathbf{F} \rightarrow \mathbf{O}$ reaction displayed the largest kinetic isotope effect (KIE, i.e. the ratio of the rates measured in $H_2O$ and $D_2O$, respectively) [31,32,35–37]. For the wild-type *Sc*CytcO the two kinetic components of the $\mathbf{F} \rightarrow \mathbf{O}$ reaction were slowed by factors of 2.5 and 2.7, respectively, while for the Glu243Asp mutant *Sc*CytcO the effect was smaller (factors of 1.7 and 1.4, respectively).

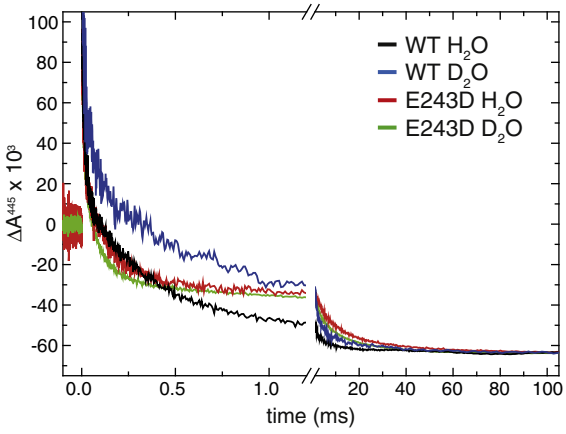


**Fig. 3.** Solvent deuterium isotope effect on the reaction of reduced *Sc*CytcO with $O_2$ as observed at 445 nm. Experimental conditions for samples in $D_2O$ after mixing: 50 mM HEPES at a pH-meter reading of 7.5, 100 μM EDTA, 0.05% DDM and 0.6 mM $O_2$. Conditions for samples in $H_2O$: 80 mM and 70 mM HEPES at pH-meter reading 7.5, for the wild-type and Glu243Asp samples, respectively, 100 μM EDTA, 0.05% DDM, and 1 mM and 0.9 mM $O_2$ for the wild type and Glu243Asp samples, respectively. The traces have been scaled to 1 μM of reacting enzyme and the traces at 445 have been multiplied by 1.35 and 1.65 for the wild type *Sc*CytcO in $H_2O$ and $D_2O$, respectively, to obtain the same reduced-oxidized total absorbance change.

## 4. Discussion

We have investigated the kinetics of electron transfer in the wild-type and Glu243Asp variant *Sc*CytcOs. The modified residue is located at the end of the D pathway and has been suggested to be a proton donor to both the pump site and the catalytic site in bacterial CytcOs. In contrast, in mitochondrial *Bt*CytcO it has been suggested that the pumped protons are transferred through a different H pathway [15,16], while the D pathway and/or K pathway are used exclusively for proton transfer from the *n* side of the membrane to the catalytic site [17].

For the wild-type *Sc*CytcO, essentially the same four kinetic components were observed as for the *Bt*CytcO and *Rs*CytcO, corresponding to a reaction sequence of:

$$\mathbf{R}\rightarrow\mathbf{A}\rightarrow\mathbf{P_R}\rightarrow\mathbf{F}\rightarrow\mathbf{O}$$

(for review, see [7,8,10,20,21]). The time constants of these reactions were also similar to those determined for other CytcOs, though with minor differences.

During the $\mathbf{P_R}\rightarrow\mathbf{F}$ reaction, ~70% of $Cu_A$ became oxidized (10% standard deviation of three measurements, see Fig. 2C, increase in absorbance over a time scale ~0–200 μs), which is slightly larger than that with the *Bt*CytcO (~60%) and *Rs*CytcO (~50%) [33]. This electron transfer arises from equilibration of an electron between $Cu_A$ and heme *a* and indicates that the midpoint potential of heme *a* is approximately ~25 mV more positive than that of $Cu_A$ (when **F** is formed at the catalytic site) for the *Sc*CytcO (the $\Delta E_m$s for the *Bt*CytcO and *Rs*CytcO were ~10 mV and 0 mV, respectively).

Binding of $O_2$, $\mathbf{P_R}$ formation and the $\mathbf{P_R}\rightarrow\mathbf{F}$ reaction in *Sc*CytcO displayed roughly the same time constants as in *Rs*CytcO and *Bt*CytcO. However, the main component of the final $\mathbf{F}\rightarrow\mathbf{O}$ step in *Sc*CytcO was faster ($\tau\cong 0.4$ ms) than that in *Bt*CytcO ($\tau\cong 1$ ms) and *Rs*CytcO ($\tau\cong 1.3$ ms) [10,33,38]. This difference in time constants is qualitatively consistent with the increased extent of electron transfer to heme *a* in the $\mathbf{P_R}\rightarrow\mathbf{F}$ step (see above) since the $\mathbf{F}\rightarrow\mathbf{O}$ reaction rate was determined, at least in part (see more detailed discussion below), by the electron distribution between $Cu_A$ and heme *a*.

Two kinetic components were associated with the $\mathbf{F}\rightarrow\mathbf{O}$ reaction of *Sc*CytcO. In the wild-type, the main component (~84%) displayed a time constant of ~0.4 ms, and the remaining ~16% displayed a time constant of ~6 ms. The minor component could originate from a sub-population of the *Sc*CytcO. However, processes that are slower than the main $\mathbf{F}\rightarrow\mathbf{O}$ oxidation phase have been observed also with other CytcOs. For example, with the *Rs*CytcO a slow proton uptake was observed over a time scale of ~5 ms after the ~1.3 ms phase of the $\mathbf{F}\rightarrow\mathbf{O}$ redox transition [33,39]. Furthermore, in an Asn139Asp mutant of *Rs*CytcO the 445 nm $\mathbf{F}\rightarrow\mathbf{O}$ absorbance changes were also biphasic and the fraction of the slow component correlated with the proton-pumping stoichiometry (unpublished data and [40]). In addition, Wikström and colleagues have suggested that the product of the reaction of CytcO with $O_2$ is a metastable "activated" state of the enzyme, which presumably spontaneously decays into the relaxed **O** state [5,41]. Such phenomena may contribute to the biphasic absorbance changes that are observed in the reaction of conversion of **F** into the stable **O** form.

With the Glu243Asp variant *Sc*CytcO the $\mathbf{P_R}\rightarrow\mathbf{F}$ reaction rate was slowed by a factor of ~3 to ~300 μs. This effect is similar to that observed for the equivalent mutation Glu286Asp in *Rs*CytcO, where the reaction was slowed by a factor of ~5 [28]. Earlier studies with bacterial CytcOs such as *Rs*CytcO have shown that the $\mathbf{P_R}\rightarrow\mathbf{F}$ rate reflects the proton transfer rate from Glu286 (Glu243 in *Sc*CytcO) to the catalytic site [27,34]. Consequently, a slower rate is qualitatively consistent with the shorter side chain of Asp, leading to a larger distance for proton transfer and/or disruption of the hydrogen-bonded proton pathway to the catalytic site. Yet another possibility is that the p$K_a$ of Asp243 is lower than that of Glu243 such that the Asp is not fully protonated at the pH of the measurement, which would also slow down the overall $\mathbf{P_R}\rightarrow\mathbf{F}$ reaction [34]. Regardless of its physical origin, the slowed $\mathbf{P_R}\rightarrow\mathbf{F}$ reaction rate in the Glu243Asp variant *Sc*CytcO indicates that the D pathway is involved in proton transfer to the catalytic site also in mitochondrial *Sc*CytcO, which is in accordance with earlier suggestions [17].

Both kinetic phases of the $\mathbf{F}\rightarrow\mathbf{O}$ reaction were also slowed in the Glu243Asp mutant *Sc*CytcO. The first of these decreased by a factor of ~5 (from ~0.4 ms in the wild-type to ~1.8 ms in the Glu243Asp mutant *Sc*CytcO), while the second decreased by a factor of ~2 (from ~6 ms with the wild-type to ~14 ms in the Glu243Asp mutant *Sc*CytcO). However, the relative fraction of the slow component increased significantly at both 445 and 830 nm (Fig. 2), increasing the overall halftime of $\mathbf{F}\rightarrow\mathbf{O}$ by a factor of ~10. Slowing of the $\mathbf{F}\rightarrow\mathbf{O}$ reaction was also observed in the corresponding Glu286Asp mutant of *Rs*CytcO, though in this case the overall time constant increased by only a factor of ~1.4. While the $\mathbf{P_R}\rightarrow\mathbf{F}$ reaction is determined by proton transfer from Glu286 (*Rs*CytcO numbering) to the catalytic site, the $\mathbf{F}\rightarrow\mathbf{O}$ determinants are more complex [6,42]. Data from earlier studies indicate that the $\mathbf{F}\rightarrow\mathbf{O}$ rate may be limited by the release of a proton that is pumped during this reaction [21,43]. In addition, as already noted above, the $\mathbf{F}\rightarrow\mathbf{O}$ rate is in part determined by the fraction of reduced heme *a* and in part by the proton-transfer rate from Glu286 (Glu243 in *Sc*CytcO) to the catalytic site. Thus, its slower rate in the Glu243Asp mutant is qualitatively consistent with slower proton transfer from Asp243 to the catalytic site and the lack of electronic equilibration from $Cu_A$ towards heme *a* during the $\mathbf{P_R}\rightarrow\mathbf{F}$ ($\tau\cong 300$ μs) reaction, compared to the wild-type *Sc*CytcO (Fig. 2C, red trace). Results from earlier studies have shown that in the wild-type CytcO this electron transfer is triggered by re-protonation of Glu286 (*R. sphaeroides* CytcO numbering) after proton transfer from Glu286 to the catalytic site [27,44]. Thus the absence of electron transfer could be due to delayed re-protonation of the Asp243 after proton transfer from Asp243 to the catalytic site. Alternatively, as outlined above, the p$K_a$ of Asp243 could be lower than that of Glu243 such that Asp243 is always unprotonated, i.e. the $\mathbf{P_R}\rightarrow\mathbf{F}$ and $\mathbf{F}\rightarrow\mathbf{O}$ reactions involve proton transfer from solution to the catalytic site, via an unprotonated Asp243.

The conclusion that the release of the pumped proton may control the $\mathbf{F}\rightarrow\mathbf{O}$ rate was in part reached on the basis of observation of a relatively large KIE of ~7 for the $\mathbf{F}\rightarrow\mathbf{O}$ reaction and specifically for the release of the pumped proton [43]. This effect was significantly larger than that for proton uptake through the D pathway (~2) [43]. For wild-type *Sc*CytcO the KIE of the $\mathbf{F}\rightarrow\mathbf{O}$ reaction was 2.5 (2.7 for the slower component), which is significantly smaller than that for the *Rs*CytcO (~7), but closer to the values obtained with the *Bt*CytcO (2.5–4, [31,35]). With the Glu243Asp variant of *Sc*CytcO an even smaller KIE of 1.7 (1.4 for the slower component) was observed (Table 1). Even though with the bacterial CytcO the large KIE may reflect events linked to the release of the pumped proton [43], a large KIE is not an essential feature of reaction steps linked to proton pumping. Nevertheless, these data show that the rate-limiting steps of the $\mathbf{P_R}\rightarrow\mathbf{F}$ and $\mathbf{F}\rightarrow\mathbf{O}$ transitions with the ScCytcO involve proton-transfer reactions and that these reactions in the ScCytcO resemble those of the mitochondrial *Bt*CytcO rather than those of the bacterial *Rs*CytcO.

## 5. Conclusions

The data from this study show that during reaction of the reduced *Sc*CytcO with $O_2$ essentially the same sequence of absorbance changes is observed as with the *Rs*CytcO and *Bt*CytcO, which indicates that the reaction proceeds along the same trajectory in all these enzymes. Significant slowing of the $\mathbf{A}\rightarrow\mathbf{P_R}$, $\mathbf{P_R}\rightarrow\mathbf{F}$ and $\mathbf{F}\rightarrow\mathbf{O}$ steps occurred upon replacement of Glu243 by Asp, which confirms that the D pathway is indeed a functional proton pathway in *Sc*CytcO. Further experiments with other variants of the yeast enzyme will be required to address its specific roles in substrate proton delivery and proton pumping.

**Table 1**
Rates and time constants (in parentheses) of the reaction steps after binding of $O_2$ to the reduced *Sc*CytcO. Two components were observed for the **F → O** reaction. The fractions of these components are given for the data obtained at 445 nm. Standard errors were typically ≤10% of the measured values (standard error, 3 measurements with different samples). In cases when larger values were obtained they are given in the table. The data obtained with the *Bt*CytcO and *Rs*CytcO are from [22,28,33,35,45,46].

| | $H_2O/D_2O$ | **A → $P_R$** | **$P_R$ → F** | **F → $O^{1st}$** | **F → $O^{2nd}$** |
|---|---|---|---|---|---|
| *Sc*CytcO WT | $H_2O$ | 44,000 $s^{-1}$ ($\tau \cong 23$ μs) | 10,800 $s^{-1}$ ($\tau \cong 90$ μs) | 2600 ± 400 $s^{-1}$ (84%) ($\tau \cong 0.4$ ms) | 160 $s^{-1}$ (16%) ($\tau \cong 6$ ms) |
| *Sc*CytcO WT | $D_2O$ | 18,000 $s^{-1}$ ($\tau \cong 55$ μs) | ND | 1100 $s^{-1}$ (80%) ($\tau \cong 0.9$ ms) | 60 $s^{-1}$ (20%) ($\tau \cong 17$ ms) |
| *Sc*CytcO Glu243Asp | $H_2O$ | 13,000 ± 2000 $s^{-1}$ ($\tau \cong 77$ μs) | 3300 $s^{-1}$ ($\tau \cong 300$ μs) | 560 ± 100 $s^{-1}$ (50%) ($\tau \cong 1.8$ ms) | 70 ± 10 $s^{-1}$ (50%) ($\tau \cong 14$ ms) |
| *Sc*CytcO Glu243Asp | $D_2O$ | 8700 $s^{-1}$ ($\tau \cong 110$ μs) | ND | 330 $s^{-1}$ (50%) ($\tau \cong 3.0$ ms) | 50 $s^{-1}$ (50%) ($\tau \cong 20$ ms) |
| *Bt*CytcO | $H_2O$ | 25–30 μs | 65–80 μs | 0.9–1.1 ms | – |
| *Bt*CytcO | $D_2O$ | 45 μs | 130 μs | 3 ms | – |
| *Rs*CytcO, WT | $H_2O$ | 30–70 μs | 110–160 μs | 1.2–1.4 ms | – |
| *Rs*CytcO, WT | $D_2O$ | 110 μs | 240 μs | 8–9 ms | – |
| *Rs*CytcO, Glu286Asp | $H_2O$ | ND | 560–800 μs | 1.8 ms | – |
| *Rs*CytcO, Glu286Asp | $D_2O$ | ND | 2 ms | 4.5 ms | – |

## References


[1] J. Hemp, R.B. Gennis, Diversity of the heme-copper superfamily in archaea: insights from genomics and structural modeling, Results Probl. Cell Differ. 45 (2008) 1–31.
[2] M.M. Pereira, M. Santana, M. Teixeira, A novel scenario for the evolution of haem-copper oxygen reductases, Biochim. Biophys. Acta, Bioenerg. 1505 (2001) 185–208.
[3] J.P. Hosler, S. Ferguson-Miller, D.A. Mills, Energy transduction: proton transfer through the respiratory complexes, Annu. Rev. Biochem. 75 (2006) 165–187.
[4] S. Yoshikawa, K. Muramoto, K. Shinzawa-Itoh, H. Aoyama, T. Tsukihara, K. Shimokata, Y. Katayama, H. Shimada, Proton pumping mechanism of bovine heart cytochrome c oxidase, Biochim. Biophys. Acta Bioenerg. 1757 (2006) 1110–1116.
[5] M. Wikström, M.I. Verkhovsky, Towards the mechanism of proton pumping by the haem-copper oxidases, Biochim. Biophys. Acta Bioenerg. 1757 (2006) 1047–1051.
[6] A. Namslauer, P. Brzezinski, Structural elements involved in electron-coupled proton transfer in cytochrome c oxidase, FEBS Lett. 567 (2004) 103–110.
[7] P. Brzezinski, R.B. Gennis, Cytochrome c oxidase: exciting progress and remaining mysteries, J. Bioenerg. Biomembr. 40 (2008) 521–531.
[8] P. Brzezinski, P. Ädelroth, Design principles of proton-pumping haem-copper oxidases, Curr. Opin. Struct. Biol. 16 (2006) 465–472.
[9] O.M.H. Richter, B. Ludwig, Electron transfer and energy transduction in the terminal part of the respiratory chain — lessons from bacterial model systems, Biochim. Biophys. Acta Bioenerg. 1787 (2009) 626–634.
[10] I. Belevich, M.I. Verkhovsky, Molecular mechanism of proton translocation by cytochrome c oxidase, Antioxid. Redox Signal. 10 (2008) 1–29.
[11] S. Ferguson-Miller, C. Hiser, J. Liu, Gating and regulation of the cytochrome c oxidase proton pump, Biochim. Biophys. Acta Bioenerg. 1817 (2012) 489–494.
[12] P.R. Rich, A. Maréchal, Functions of the hydrophilic channels in protonmotive cytochrome c oxidase, J. R. Soc. Interface 10 (2013).
[13] A. Maréchal, B. Meunier, D. Lee, C. Orengo, P.R. Rich, Yeast cytochrome c oxidase: a model system to study mitochondrial forms of the haem-copper oxidase superfamily, Biochim. Biophys. Acta Bioenerg. 1817 (2012) 620–628.
[14] B. Meunier, A. Maréchal, P.R. Rich, Construction of histidine-tagged yeast mitochondrial cytochrome c oxidase for facile purification of mutant forms, Biochem. J. 444 (2012) 199–204.
[15] S. Yoshikawa, K. Muramoto, K. Shinzawa-Itoh, Proton-pumping mechanism of cytochrome c oxidase, Annu. Rev. Biophys. Biomol. Struct. 40 (2011) 205–223.
[16] S. Yoshikawa, K. Muramoto, K. Shinzawa-Itoh, The $O_2$ reduction and proton pumping gate mechanism of bovine heart cytochrome c oxidase, Biochim. Biophys. Acta Bioenerg. 1807 (2011) 1279–1286.
[17] S. Yoshikawa, K. Muramoto, K. Shinzawa-Itoh, M. Mochizuki, Structural studies on bovine heart cytochrome c oxidase, Biochim. Biophys. Acta Bioenerg. 1817 (2012) 579–589.
[18] H.M. Lee, T.K. Das, D.L. Rousseau, D. Mills, S. Ferguson-Miller, R.B. Gennis, Mutations in the putative H-channel in the cytochrome c oxidase from *Rhodobacter sphaeroides* show that this channel is not important for proton conduction but reveal modulation of the properties of heme a, Biochemistry 39 (2000) 2989–2996.
[19] J. Salje, B. Ludwig, O.M. Richter, Is a third proton-conducting pathway operative in bacterial cytochrome c oxidase? Biochem. Soc. Trans. 33 (2005) 829–831.
[20] Ó. Einarsdóttir, Fast reactions of cytochrome-oxidase, Biochim. Biophys. Acta 1229 (1995) 129–147.
[21] V.R.I. Kaila, M.I. Verkhovsky, M. Wikström, Proton-coupled electron transfer in cytochrome oxidase, Chem. Rev. 110 (2010) 7062–7081.
[22] P. Brzezinski, L.N. Öjemyr, P. Ädelroth, Intermediates generated during the reaction of reduced *Rhodobacter sphaeroides* cytochrome c oxidase with dioxygen, Biochim. Biophys. Acta Bioenerg. 1827 (2013) 843–847.
[23] K. Faxén, G. Gilderson, P. Ädelroth, P. Brzezinski, A mechanistic principle for proton pumping by cytochrome c oxidase, Nature 437 (2005) 286–289.
[24] M.I. Verkhovsky, J.E. Morgan, M.L. Verkhovskaya, M. Wikström, Translocation of electrical charge during a single turnover of cytochrome-c oxidase, Biochim. Biophys. Acta 1318 (1997) 6–10.
[25] P. Ädelroth, M. Svensson Ek, D.M. Mitchell, R.B. Gennis, P. Brzezinski, Glutamate 286 in cytochrome aa3 from *Rhodobacter sphaeroides* is involved in proton uptake during the reaction of the fully-reduced enzyme with dioxygen, Biochemistry 36 (1997) 13824–13829.
[26] E.A. Gorbikova, I. Belevich, M. Wikström, M.I. Verkhovsky, The proton donor for O–O bond scission by cytochrome c oxidase, Proc. Natl. Acad. Sci. U. S. A. 105 (2008) 10733–10737.
[27] I.A. Smirnova, P. Ädelroth, R.B. Gennis, P. Brzezinski, Aspartate-132 in cytochrome c oxidase from *Rhodobacter sphaeroides* is involved in a two-step proton transfer during oxo-ferryl formation, Biochemistry 38 (1999) 6826–6833.
[28] P. Ädelroth, M. Karpefors, G. Gilderson, F.L. Tomson, R.B. Gennis, P. Brzezinski, Proton transfer from glutamate 286 determines the transition rates between oxygen intermediates in cytochrome c oxidase, Biochim. Biophys. Acta 1459 (2000) 533–539.
[29] U. Pfitzner, A. Odenwald, T. Ostermann, L. Weingard, B. Ludwig, O.M.H. Richter, Cytochrome c oxidase (Heme $aa_3$) from *Paracoccus denitrificans*: analysis of mutations in putative proton channels of subunit I, J. Bioenerg. Biomembr. 30 (1998) 89–97.
[30] M.L. Verkhovskaya, A. García-Horsman, A. Puustinen, J.L. Rigaud, J.E. Morgan, M.I. Verkhovsky, M. Wikström, Glutamic acid 286 in subunit I of cytochrome bo3 is involved in proton translocation, Proc. Natl. Acad. Sci. U. S. A. 94 (1997) 10128–10131.
[31] M. Karpefors, P. Ädelroth, P. Brzezinski, The onset of the deuterium isotope effect in cytochrome c oxidase, Biochemistry 39 (2000) 5045–5050.
[32] M. Karpefors, P. Ädelroth, A. Aagaard, I.A. Smirnova, P. Brzezinski, The deuterium isotope effect as a tool to investigate enzyme catalysis: proton-transfer control mechanisms in cytochrome c oxidase, Isr. J. Chem. 39 (1999) 427–437.
[33] P. Ädelroth, M. Ek, P. Brzezinski, Factors determining electron-transfer rates in cytochrome *c* oxidase: investigation of the oxygen reaction in the *R. sphaeroides* and bovine enzymes, Biochim. Biophys. Acta 1367 (1998) 107–117.
[34] A. Namslauer, A. Aagaard, A. Katsonouri, P. Brzezinski, Intramolecular proton-transfer reactions in a membrane-bound proton pump: the effect of pH on the peroxy to ferryl transition in cytochrome c oxidase, Biochemistry 42 (2003) 1488–1498.
[35] S. Hallén, T. Nilsson, Proton transfer during the reaction between fully reduced cytochrome c oxidase and dioxygen: pH and deuterium isotope effects, Biochemistry 31 (1992) 11853–11859.
[36] S.A. Siletsky, A.S. Pawate, K. Weiss, R.B. Gennis, A.A. Konstantinov, Transmembrane charge separation during the ferryl-oxo-> oxidized transition in a nonpumping mutant of cytochrome c oxidase, J. Biol. Chem. 279 (2004) 52558–52565.
[37] M. Karpefors, P. Ädelroth, P. Brzezinski, Localized control of proton transfer through the D-pathway in cytochrome c oxidase: application of the proton-inventory technique, Biochemistry 39 (2000) 6850–6856.
[38] Ó. Einarsdóttir, I. Szundi, Time-resolved optical absorption studies of cytochrome oxidase dynamics, Biochim. Biophys. Acta Bioenerg. 1655 (2004) 263–273.
[39] P. Brzezinski, P. Ädelroth, Pathways of proton transfer in cytochrome c oxidase, J. Bioenerg. Biomembr. 30 (1998) 99–107.
[40] A. Namslauer, A.S. Pawate, R.B. Gennis, P. Brzezinski, Redox-coupled proton translocation in biological systems: proton shuttling in cytochrome c oxidase, Proc. Natl. Acad. Sci. U. S. A. 100 (2003) 15543–15547.
[41] D. Bloch, I. Belevich, A. Jasaitis, C. Ribacka, A. Puustinen, M.I. Verkhovsky, M. Wikström, The catalytic cycle of cytochrome c oxidase is not the sum of its two halves, Proc. Natl. Acad. Sci. U. S. A. 101 (2004) 529–533.
[42] S. Paula, A. Sucheta, I. Szundi, Ó. Einarsdóttir, Proton and electron transfer during the reduction of molecular oxygen by fully reduced cytochrome c oxidase: a flow-flash investigation using optical multichannel detection, Biochemistry 38 (1999) 3025–3033.

[43] L. Salomonsson, K. Faxén, P. Ädelroth, P. Brzezinski, The timing of proton migration in membrane-reconstituted cytochrome c oxidase, Proc. Natl. Acad. Sci. U. S. A. 102 (2005) 17624–17629.
[44] M. Karpefors, P. Ädelroth, Y. Zhen, S. Ferguson-Miller, P. Brzezinski, Proton uptake controls electron transfer in cytochrome c oxidase, Proc. Natl. Acad. Sci. U. S. A. 95 (1998) 13606–13611.
[45] L. Salomonsson, G. Brändén, P. Brzezinski, Deuterium isotope effect of proton pumping in cytochrome c oxidase, Biochim. Biophys. Acta Bioenerg. 1777 (2008) 343–350.
[46] D. Zaslavsky, R.C. Sadoski, K. Wang, B. Durham, R.B. Gennis, F. Millett, Single electron reduction of cytochrome c oxidase compound F: resolution of partial steps by transient spectroscopy, Biochemistry 37 (1998) 14910–14916.